Simple fabrication of silicon nanowires by zinc-thermal reduction of silicon tetrachloride at 773 K

Yusaku Nishimura[†], Toshiyuki Nohira*, Yohsuke Mizutani, and Rika Hagiwara

Graduate School of Energy Science, Kyoto University, Yoshida-hommachi, Sakyo-ku, Kyoto 606-8501, Japan

*Corresponding author: nohira@energy.kyoto-u.ac.jp

[†]Present address: Materials Analysis & Evaluation Division, Toyota Central R&D Labs, Inc., 41-1 Yokomichi, Nagakute, Aichi 480-1192, Japan.

Silicon nanowires (SiNWs) have been a target of intensive research because of their unique properties[1–4] and prospective applications[4–6]. New SiNW production processes that are more suitable for industrial and/or laboratory scales are strongly needed, because the conventional processes require complex apparatuses and/or procedures. Here, we report a simple SiNW production process based on zinc-thermal reduction of $SiCl_4$ in a sealed Pyrex tube at 773 K. Without using a catalyst, SiNWs with a diameter of about 300 nm were produced. The SiNWs consisted of mainly an amorphous phase, but also included a minor microcrystalline component. The introduction of Au nanoparticles to the reaction tube wall facilitated crystallization and resulted in the growth of thinner SiNWs. The typical

diameter of these SiNWs was 10–20 nm. The simple apparatus and low operating temperature of this new process is advantageous in producing SiNWs on both industrial and laboratory scales.

Silicon nanowires are notable for their potential applications, such as SiNW-array solar cells[4], thermoelectric devices[5], and negative electrodes for Li-ion batteries[6]. The leading processes of bottom-up fabrication (e.g., the vapor–liquid–solid (VLS) process[7] and the solution–liquid–solid (SLS) process[1]) utilize droplets of metal catalysts such as Au and Ag for SiNW growth. The Si sources in these processes are laser ablation of bulk Si[7], decomposition of polysilane[1], or reduction of $SiCl_4$ by Na[8] or H_2[9]. On the other hand, chemical etching[10] is a leading top-down fabrication process, where Si wafers are etched to form nanowires with assistance from metal catalysts. Although these conventional processes are relatively successful, new production processes that require less complex apparatuses and can avoid the risk of contamination by catalysts or solvents are highly desirable.

The authors believed that zinc-thermal reduction of $SiCl_4$ represented a promising SiNW production process. The zinc-thermal reduction of $SiCl_4$ was first reported by Lyon et al. in 1949 for the production of high-purity Si[11]. Recently, the process has been intensively researched for the mass production of solar-grade Si[12,13]. It is well known that the zinc-thermal reduction of $SiCl_4$ at 1073–1273 K produces Si fibers of micrometer-scale diameter[14]. The authors expected that this diameter could be reduced to a nanometer scale by lowering the reaction temperature to around 773 K. This lowering of the temperature significantly enlarged the range of available materials for both apparatus and substrate. For example, steel and Pyrex can be used at 773 K, but not above 1073 K. Moreover, the low-temperature process consumes less energy. More

recently, Uesawa et al. reported that crystalline SiNWs can be produced by zinc-thermal reduction of $SiCl_4$ at 1193–1283 K[15]. However, this higher process temperature restricts the available materials and consumes more energy.

In this study, the fabrication of SiNWs was conducted by a very simple process. $SiCl_4$ and Zn were sealed in a Pyrex tube and heated to 773 K (Figs. 1a and 1b). Further efforts were devoted to reducing the diameter of SiNWs by introducing Au nanoparticles (AuNPs) similar to those used in the VLS and the SLS processes, as described later (Fig. 1c).

As can be seen in Fig. 1b, a dark-brown powder was produced on the tube walls. According to the literature[16,17], nanostructured Si, such as nanowires and nanoparticles, has a dark-brown color. Figures 2a and 2b show SEM images of the dark-brown substance captured at different magnifications. The lower-magnification image (Fig. 2a) revealed that the substance consisted of uniform nanowires. At a higher magnification (Fig. 2b), it was found that the SiNWs had an average diameter of approximately 300 nm. In addition, the surface of the SiNWs appeared to be rough, suggesting that the formation mechanism was different from that of the VLS method. Figure 2c shows an EDX spectrum of the SiNWs. Impurities such as Zn and Cl were not detected in the SiNWs. Their microscopic structure and crystallinity were further investigated by TEM and SAED, as shown in Fig. 3a. The SiNW was comprised of two parts with different appearances: dark domains 5–20 nm in size and larger gray regions. The ED pattern indicated that the dark domains corresponded to crystalline Si, and the gray regions were amorphous Si. Therefore, the produced SiNWs were composed mainly of amorphous Si and partly of nano-crystalline Si. Micro-Raman spectroscopy was performed to evaluate the crystallinity of the SiNWs. As shown in Fig. 3b, a major broad peak centered at 480 cm^{-1} was observed, and a small sharp peak was superimposed at 520 cm^{-1}. There were also two small broad peaks around 300 cm^{-1} and

400 cm^{-1}. According to the literature[18–20], crystalline Si has a sharp peak assigned to optical phonons centered at 520 cm^{-1}. On the other hand, amorphous Si has broad peaks: one assigned to the transverse-optical phonon near 480 cm^{-1}, another assigned to the longitudinal-optical phonon around 400 cm^{-1}, and the other assigned to the longitudinal-acoustic phonon around 300 cm^{-1}. Their peak locations and broadness are due to the lack of long-range order and the relaxation of momentum conservation. Furthermore, for crystalline Si nanostructures, phonon confinement effects cause not only a red-shift of the peak, but also asymmetric peak broadening[21,22]. Therefore, Raman spectroscopy confirmed that the SiNWs consisted mainly of amorphous Si and partly of nano-crystalline Si. Amorphous SiNWs are considered to be favorable for the application as an anode material for Li-ion batteries[23].

Zinc-thermal reduction has been widely investigated for the mass production of solar-grade Si and can be expressed as[11–14]

$$SiCl_4(g) + 2\,Zn(g) \rightarrow Si(s) + 2\,ZnCl_2(g) \quad (1)$$

Since the typical operation temperature is 1073–1273 K during solar-grade Si production, few studies of zinc-thermal reduction at 773 K have been performed, and there has been no report on the formation mechanism of SiNWs at 773 K. Figure 4 shows our explanation of the SiNW formation mechanism at 773 K. As shown in Fig. 4a, the gasification of $SiCl_4$ (b.p. 331 K) occurs, followed by the melting of Zn (m.p. 693 K). Then, the reaction of $SiCl_4$ and Zn vapor begins in the vicinity of liquid Zn. Since the vapor pressure of Zn is relatively low at 773 K, approximately 1.5×10^2 Pa, the reaction front gradually progresses along the tube wall from the bottom to the top. The formation of SiNWs at the tube wall is schematically shown in Fig. 4b. As is often observed during CVD, the initial deposition of Si particles occurs preferentially at a solid substrate, which was the tube wall in the present case. Then, the produced Si

particles serve as a catalyst for subsequent reaction. Considering the low vapor pressure of Zn, the reaction sites were in a state of Zn depletion, causing the Si to grow toward the bulk in the shape of nanowires.

As described above, SiNWs were formed by zinc-thermal reduction of $SiCl_4$ at 773 K without a catalyst. However, the diameter of the SiNW was relatively large (about 300 nm). To reduce the diameter of SiNWs in the same manner as in the VLS process, AuNPs were introduced to the tube sidewall as a catalyst. After heating to 773 K, a large amount of brown substance was deposited on the tube sidewall (Fig. 1c). Figures 5a and 5b show SEM images of the brown deposits, in which SiNWs 10–100 nm in diameter, but typically 20–30 nm in diameter, were observed. According to EDX analysis (Supplementary Fig. S1), a distinct peak of the Au Mα line was observed only at the tip of the SiNWs. This suggests that the AuNPs did act as catalysts, in the same manner as in the VLS process.

The microscopic structure and crystallinity of SiNWs produced in the presence of AuNPs were also investigated. Figure 5c shows a TEM image and an SAED pattern obtained from these samples. The diameter of the SiNWs was approximately 10 nm, and the crystallinity was very high. The formation of crystalline SiNWs was further supported by micro-Raman spectroscopy, as shown in Fig. 5d, because a prominent peak centered at 520 cm^{-1}, which was assigned to crystalline Si, was clearly observed.

Although the addition of AuNPs is not practical for large-scale production because of their high cost, other inexpensive catalysts such as Al, In, and Sn[24] may also be effective for the present Zn–$SiCl_4$ system.

Methods

Liquid $SiCl_4$ (purity: 99.9%, Wako Pure Chemical Industries, Ltd.) and Zn grains (purity: 99.9%, diameter: 75–150 μm, Wako Pure Chemical Industries, Ltd.) were introduced to a Pyrex tube (1 cm in diameter and 10 cm in length) in a glove box or glove bag filled with high-purity Ar gas. Typical amounts of $SiCl_4$ and Zn were 0.2 mL (1.7×10^{-3} mol) and 0.4 g (6.1×10^{-3} mol), respectively. In some experiments, AuNPs (diameter: 20–30 μm, Sumitomo Electric Industries, Ltd.) were placed on the inner wall of the glass tube beforehand. Then, the glass tube was sealed with a gas burner and placed in an electric furnace. The glass tube was heated to 773 K for 48 hours. After cooling, the tube was cut, and a powdery substance was scraped from the inner wall and rinsed with distilled water and ethanol. The dried powder was then characterized and analyzed by the following methods.

First, the morphology of the substance was observed with a field-emission-type scanning electron microscope (FE-SEM, JEOL Ltd., JSM-6500F). Energy-dispersive X-ray spectroscopy (EDX, JEOL Ltd., JSM-6500FE) was performed to investigate the composition of the observed substance. The microscopic structure and the crystallinity of the produced SiNWs were studied by transmission electron microscopy (TEM, Hitachi, H-9000UHR) and selected area electron diffraction (SAED), respectively. Local analysis was carried out by micro-Raman spectroscopy (Horiba Jobin Yvon Inc., Labram010) using a He–Ne laser (632.8 nm). It should be noted that the micro-Raman spectroscopic analysis of the reaction product was conducted directly through the tube wall before cutting and exposing the sample to air. Laser heating during the measurement could cause not only the crystallization of an initially amorphous substance, but also an anharmonic thermal effect on the peak shape. Therefore, the temperature at the measurement point was estimated from the intensity ratio of Stokes to anti-Stokes scattering and the laser output was carefully adjusted so as not to heat up the measurement point.

References

1 Heitsch, A. T., Fanfair, D. D., Tuan, H.-Y. & Korgel, B. A. Solution-liquid-solid (SLS) growth of silicon nanowires. *Journal of the American Chemical Society* **130**, 5436-5437 (2008).

2 Lu, W. & Lieber, C. M. Semiconductor nanowires. *Journal of Physics D: Applied Physics* **39**, R387-R406 (2006).

3 Ball, P. Silicon in optoelectronics. Let there be light. *Nature* **409**, 974-976 (2001).

4 Tsakalakos, L. *et al.* Silicon nanowire solar cells. *Applied Physics Letters* **91**, 233117/233111-233117/233113 (2007).

5 Shi, L., Yao, D., Zhang, G. & Li, B. Size dependent thermoelectric properties of silicon nanowires. *Applied Physics Letters* **95**, 063102/063101-063102/063103 (2009).

6 Chan, C. K. *et al.* High-performance lithium battery anodes using silicon nanowires. *Nature Nanotechnology* **3**, 31-35 (2008).

7 Morales, A. M. & Lieber, C. M. A laser ablation method for the synthesis of crystalline semiconductor nanowires. *Science (Washington, D. C.)* **279**, 208-211 (1998).

8 Wang, C., Jiang, Y., Li, G. & Zhang, Z. A wurtz-like reaction to silicon nanowires. *Materials Letters* **62**, 2497-2499 (2008).

9 Hochbaum, A. I., Fan, R., He, R. & Yang, P. Controlled growth of Si nanowire arrays for device integration. *Nano Lett.* **5**, 457-460 (2005).

10 Huang, Z. *et al.* Extended arrays of vertically aligned sub-10 nm diameter [100] Si nanowires by metal-assisted chemical etching. *Nano letters* **8**, 3046-3051 (2008).

11 Lyon, D. W., Olson, C. M. & Lewis, E. D. Preparation of hyper-pure silicon. *Journal of the Electrochemical Society* **96**, 359-363 (1949).

12 Honda, S., Yasueda, M., Hayashida, S., Yamaguchi, M. & Tanaka, T. Production process for high purity polycrystal silicon and production apparatus for the same. US Patent 2007123011 (2007).

13 Yasuda, K. & Okabe, T. H. Production processes of solar grade silicon based on metallothermic reduction. *Nippon Kinzoku Gakkaishi* **74**, 1-9 (2010).

14 Johnson, E. R. & Amick, J. A. Formation of single-crystal silicon fibers. *Journal of Applied Physics* **25**, 1204-1205 (1954).

15 Uesawa, N., Inasawa, S., Tsuji, Y. & Yamaguchi, Y. Gas-Phase Synthesis of Rough Silicon Nanowires via the Zinc Reduction of Silicon Tetrachloride. *Journal of Physical Chemistry C* **114**, 4291-4296 (2010).

16 Nohira, T., Yasuda, K. & Ito, Y. Pinpoint and bulk electrochemical reduction of insulating silicon dioxide to silicon. *Nature Materials* **2**, 397-401 (2003).

17 Scriba, M. R., Arendse, C., Haerting, M. & Britton, D. T. Hot-wire synthesis of Si nanoparticles. *Thin Solid Films* **516**, 844-846 (2008).

18 Zwick, A. & Carles, R. Multiple-order Raman scattering in crystalline and amorphous silicon. *Physical Review B: Condensed Matter and Materials Physics* **48**, 6024-6032 (1993).
19 Temple, P. A. & Hathaway, C. E. Multiphonon Raman spectrum of silicon. *Physical Review B: Solid State* **7**, 3685-3697 (1973).
20 Brodsky, M. H., Cardona, M. & Cuomo, J. J. Infrared and Raman spectra of the silicon-hydrogen bonds in amorphous silicon prepared by glow discharge and sputtering. *Physical Review B: Solid State* **16**, 3556-3571 (1977).
21 Richter, H., Wang, Z. P. & Ley, L. The one phonon Raman spectrum in microcrystalline silicon. *Solid State Communications* **39**, 625-629 (1981).
22 Campbell, I. H. & Fauchet, P. M. The effects of microcrystal size and shape on the one phonon Raman spectra of crystalline semiconductors. *Solid State Communications* **58**, 739-741 (1986).
23 Hatchard, T. D. & Dahn, J. R. In Situ XRD and Electrochemical Study of the Reaction of Lithium with Amorphous Silicon. *Journal of the Electrochemical Society* **151**, A838-A842 (2004).
24 Yu, L. *et al.* Plasma-enhanced low temperature growth of silicon nanowires and hierarchical structures by using tin and indium catalysts. *Nanotechnology* **20**, 225604 (2009).

Figure Legends

Figure 1. Photographs of (a) the original Pyrex tube containing $SiCl_4$ and Zn grains, (b) the same tube after heating at 773 K for 48 hours. In (c), Au nano-particles were placed on the inner wall of the glass tube beforehand.

Figure 2. (a), (b) SEM images of SiNWs produced by zinc-thermal reduction of $SiCl_4$ at 773 K taken at different magnifications. (c) An EDX spectrum of SiNWs.

Figure 3. (a) A TEM image (inset: an SAED pattern) and (b) a Raman spectrum of SiNWs produced by zinc-thermal reduction of $SiCl_4$ at 773 K.

Figure 4. A formation mechanism of SiNWs by zinc-thermal reduction of $SiCl_4$ in a sealed glass tube at 773 K. (a) The phase change of materials during the

heating process and the progress of SiNW formation at 773 K. (b) A schematic representation of SiNW formation at the tube wall.

Figure 5. (a), (b) SEM images at different magnifications, (c) a TEM image (inset: an SAED pattern) and (d) a Raman spectrum of SiNWs produced by zinc-thermal reduction of $SiCl_4$ in the presence of AuNPs at 773 K.

Figure S1. An EDX spectrum measured at the tip of a SiNW that was produced by zinc-thermal reduction of $SiCl_4$ in the presence of AuNPs at 773 K.

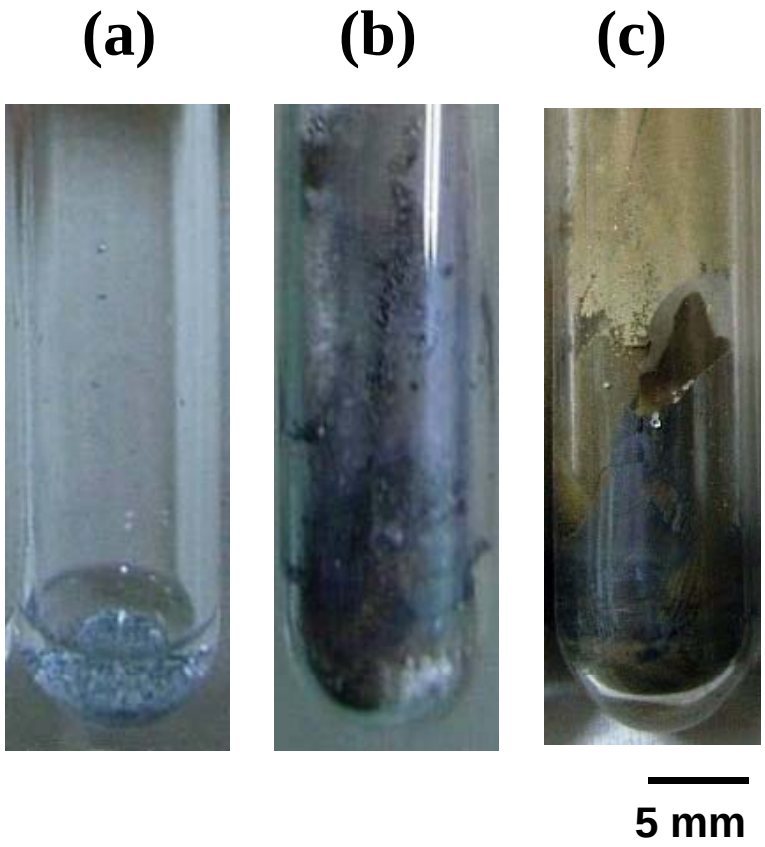

Figure 1. Photographs of (a) the original Pyrex tube containing $SiCl_4$ and Zn grains, (b) the same tube after heating at 773 K for 48 hours. In (c), Au nano-particles were placed on the inner wall of the glass tube beforehand.

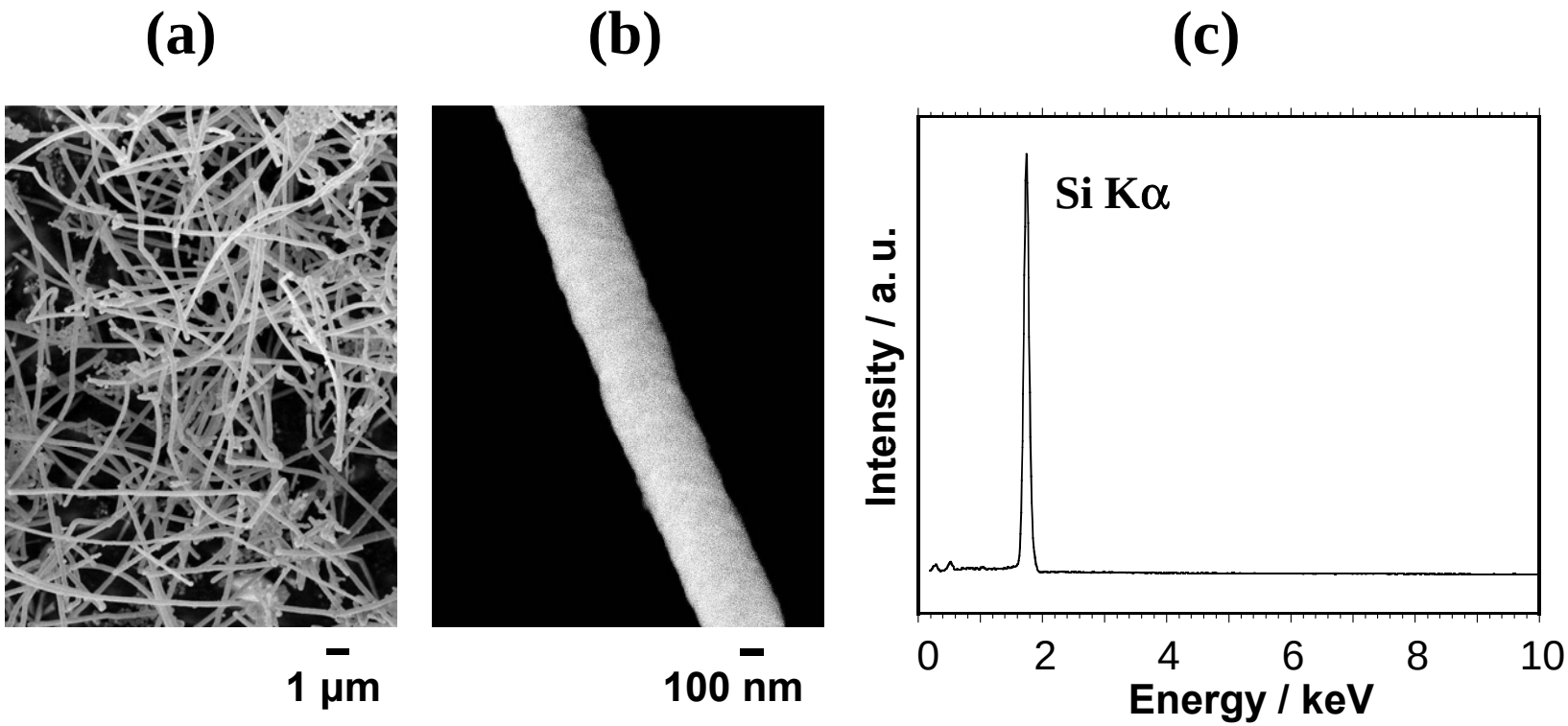

Figure 2. (a), (b) SEM images of SiNWs produced by zinc-thermal reduction of $SiCl_4$ at 773 K taken at different magnifications. (c) An EDX spectrum of SiNWs.

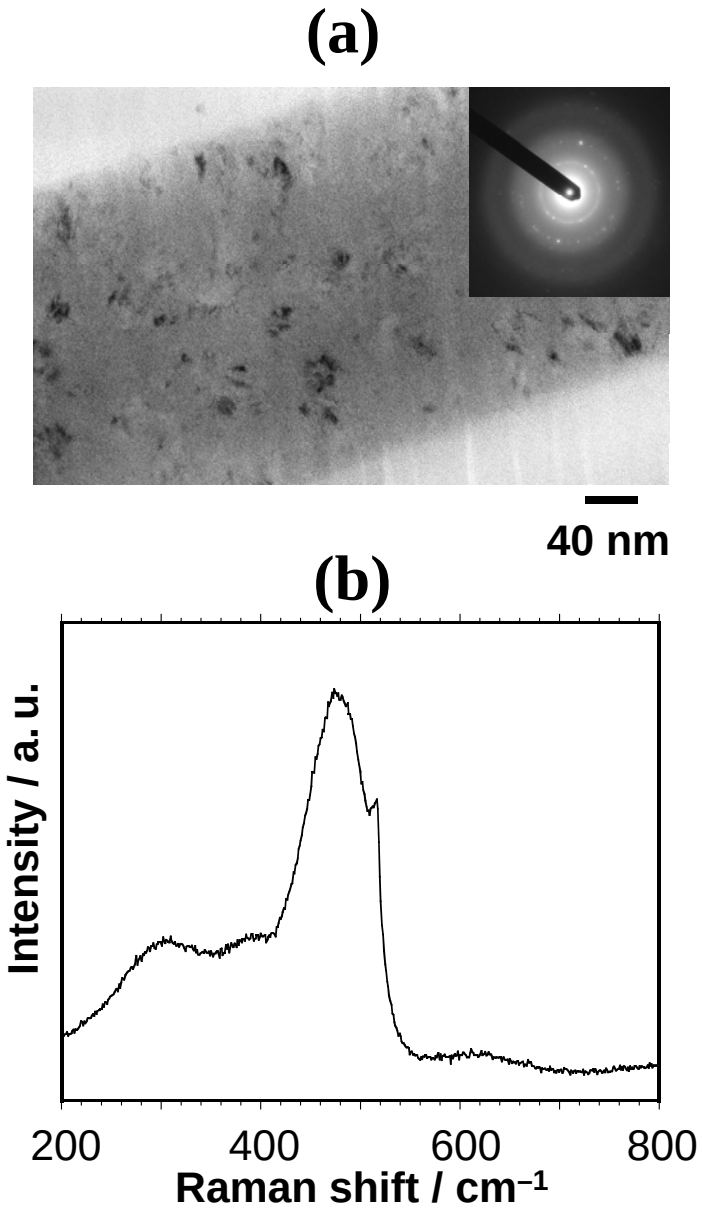

Figure 3. (a) A TEM image (inset: an SAED pattern) and (b) a Raman spectrum of SiNWs produced by zinc-thermal reduction of $SiCl_4$ at 773 K.

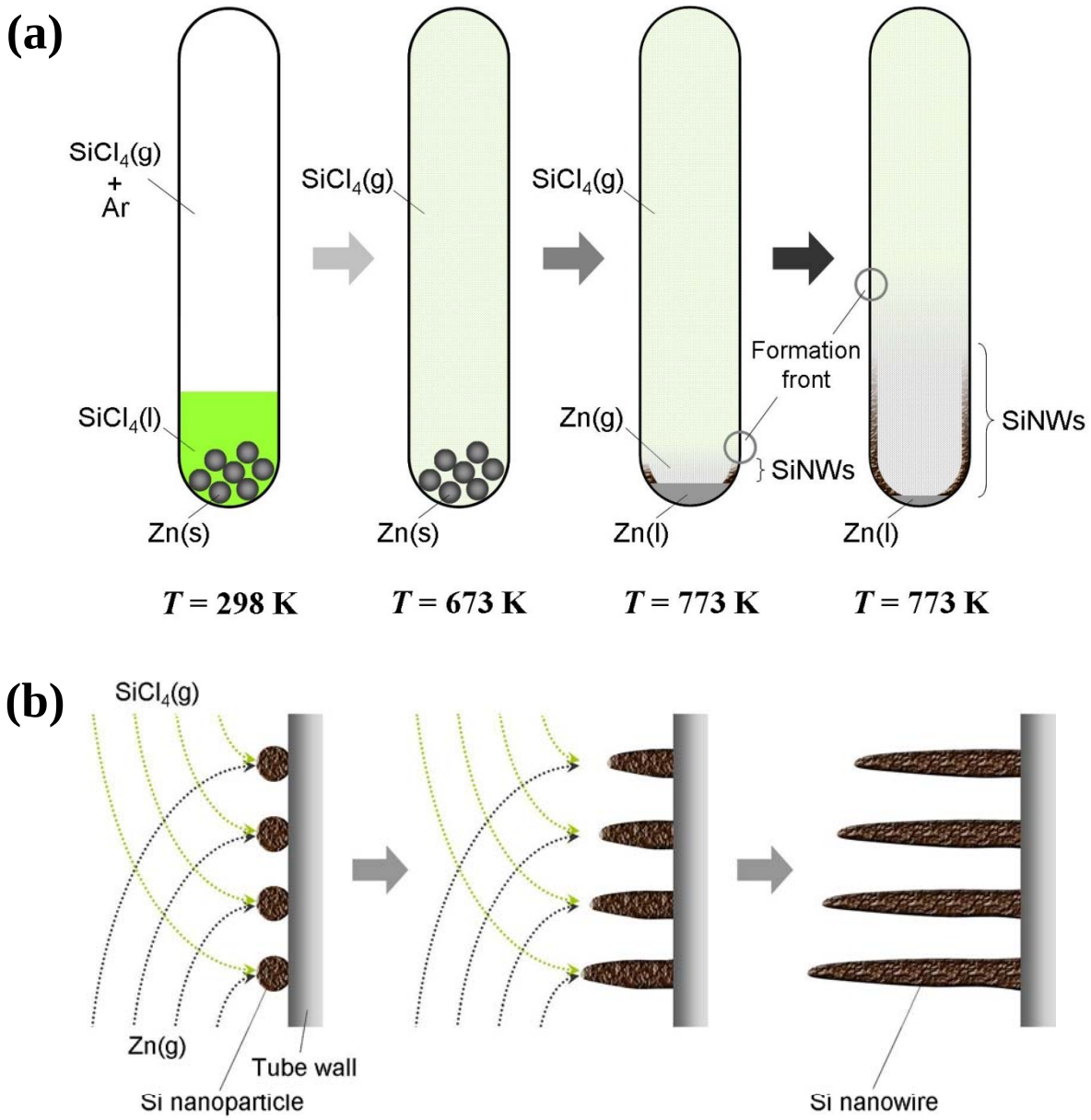

Figure 4. A formation mechanism of SiNWs by zinc-thermal reduction of $SiCl_4$ in a sealed glass tube at 773 K. (a) The phase change of materials during the heating process and the progress of SiNW formation at 773 K. (b) A schematic representation of SiNW formation at the tube wall.

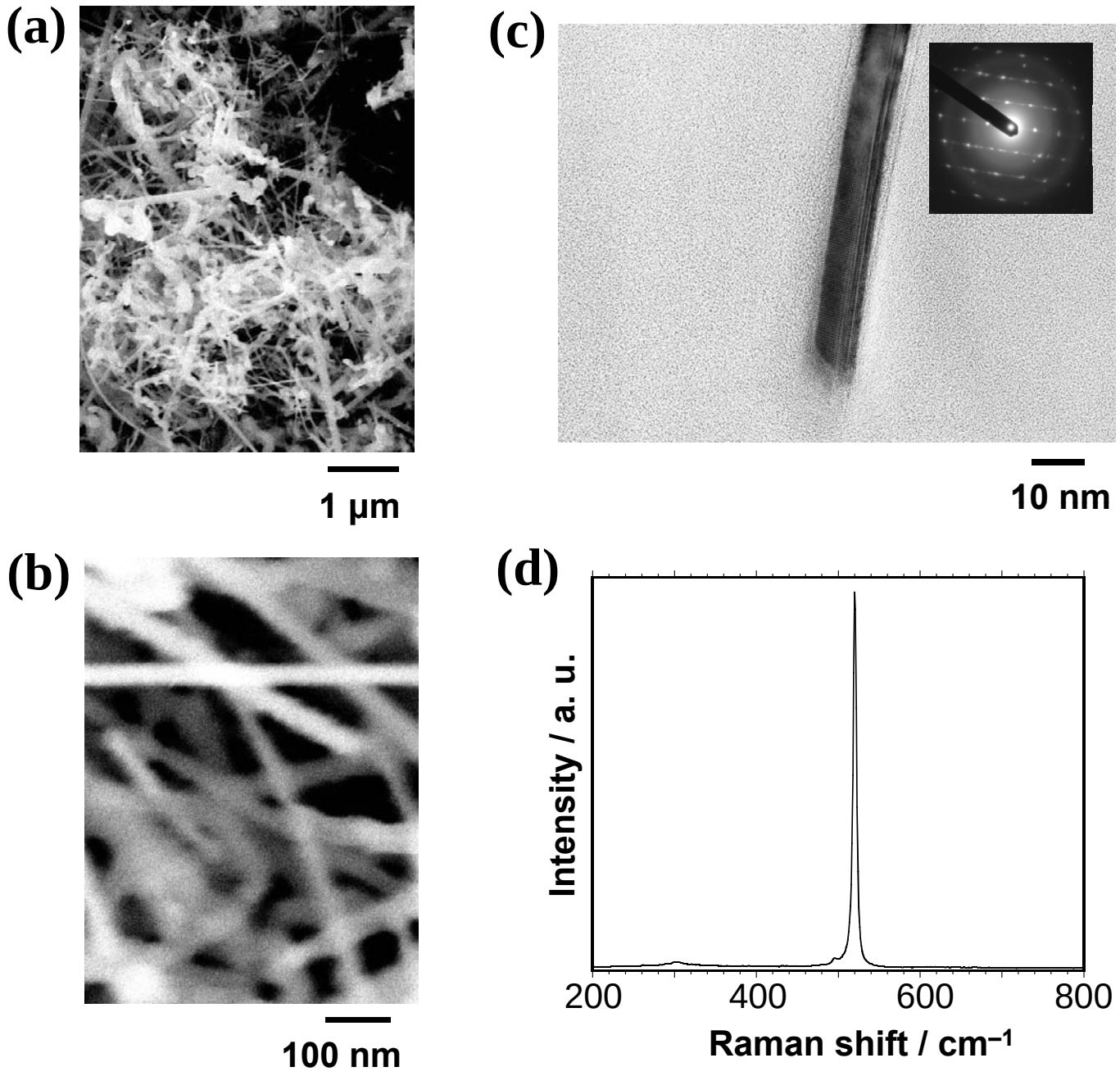

Figure 5. (a), (b) SEM images at different magnifications, (c) a TEM image (inset: an SAED pattern) and (d) a Raman spectrum of SiNWs produced by zinc-thermal reduction of $SiCl_4$ in the presence of AuNPs at 773 K.

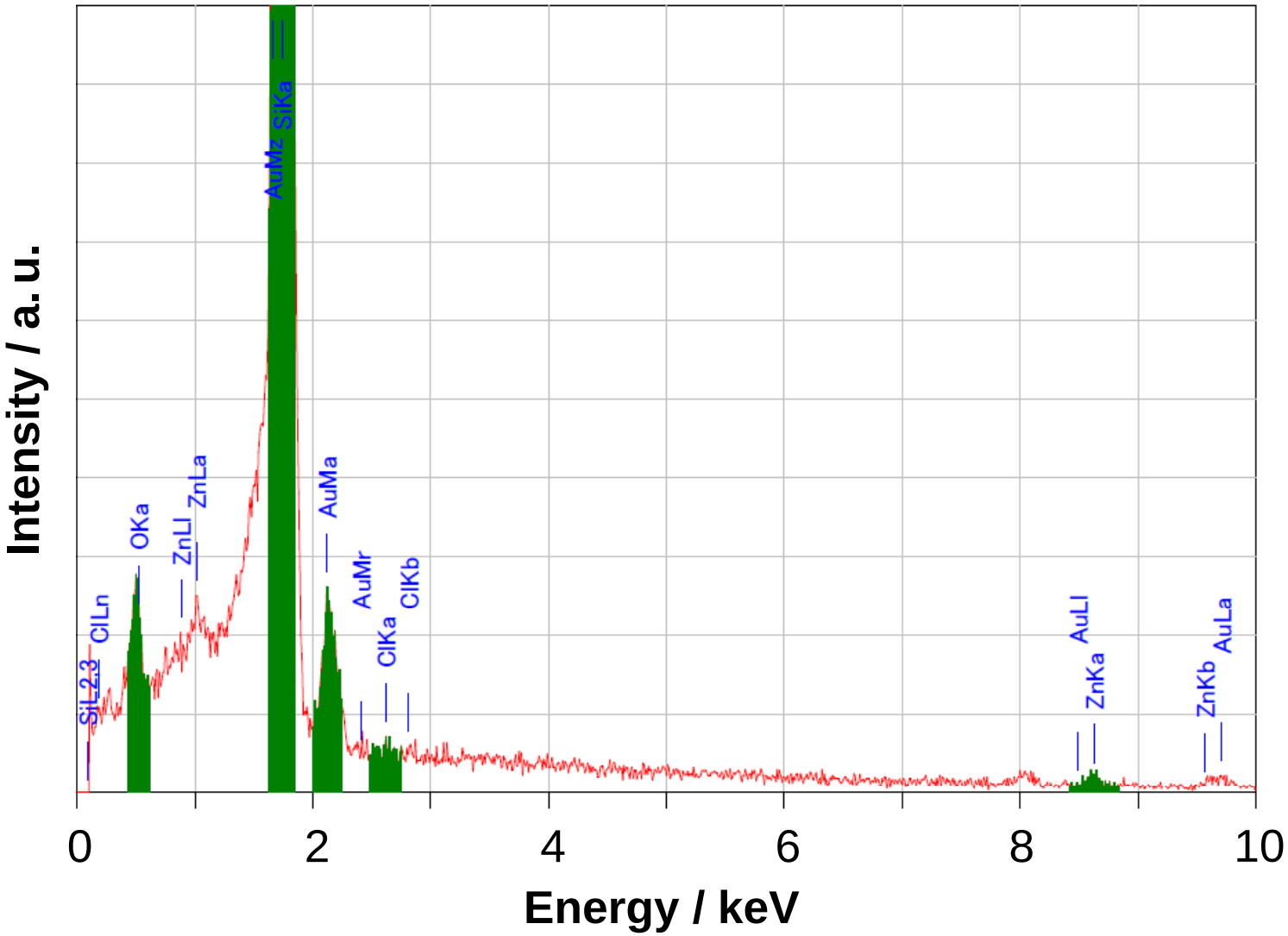

Figure S1. An EDX spectrum measured at the tip of a SiNW that was produced by zinc-thermal reduction of $SiCl_4$ in the presence of AuNPs at 773 K.